Architectural Design and Support for Knowledge Sharing Across Heterogeneous MAST systems

Ronald C. Arkin, Sergio Garcia-Vergara, Sung G. Lee

Mobile Robot Laboratory, Georgia Institute of Technology, Atlanta, GA, U.S.A.

ABSTRACT

A novel approach for the sharing of knowledge between widely heterogeneous robotic agents is presented, drawing upon Gardenfors Conceptual Spaces approach [4]. The target microrobotic platforms considered are computationally, power, sensor, and communications impoverished compared to more traditional robotics platforms due to their small size. This produces novel challenges for the system to converge on an interpretation of events within the world, in this case specifically focusing on the task of recognizing the concept of a biohazard in an indoor setting.

Keywords: Knowledge sharing, Conceptual Spaces, heterogeneous robots

1. INTRODUCTION

In research as part of the Army Research Laboratory's Collaborative Technology Alliance for MicroAutonomous Systems Technology (MAST), we are developing foundational capabilities to provide knowledge sharing across widely heterogeneous robotic platforms: small crawlers equipped with relatively exotic sensing such as airflow sensors and micro gas chromatographs; and microflyers fitted with millimeter wave radar and infrared imagers. The research question we are pursuing is how can such robotic systems with such radically different views of the world share information in ways that allow for effective distributed mission tasking and completion?

We continue to exploit our novel approach to this problem that leverages our significant prior work [6-10] in the conceptual spaces framework developed by Gardenfors [4,1]. In this paper we focus on the architectural design and implementation issues associated with widely heterogeneous micro-robots that are tasked for specific missions. This involves the creation of an abstract sensor layer, which is mapped onto a platform-specific conceptual space that defines real-world objects in the context of the sensory capacity of each robotic agent. These in turn communicate high-level symbolic concepts along with a robot identification (id) and target location couched in an egocentric or allocentric (landmark-centered) frame of reference. For MAST we have considered a range of mission scenarios in the past [14] but the specific mission considered for the research in this paper involves multi-robot search, detection, and operator alert for possible biohazards or chemical weapons within an interior structure using teams of microflyers and crawlers equipped with highly disparate and somewhat esoteric sensor suites.

Our technical approach involves the following major thrust areas:

1. Extending the conceptual spaces approach for knowledge sharing among heterogeneous team members, focusing on the constraints imposed in MAST regarding power, sensing, computation, and communication.

2. Within the architecture, to develop suitable MAST behaviors for the flyers and crawlers operating within the defined mission context to efficiently exploit shared knowledge based upon data derived or simulated from MAST-specific sensors under development by the Microsystems group.

Of necessity, as these flyers, crawlers, and sensors are currently under development by other MAST team members we are using surrogate robotic platforms and sensors to test these ideas.

2. OVERVIEW ON CONCEPTUAL SPACES

Gärdenfors' Conceptual Space Theory [4] suggests a metric world of thought that represents objects and abstract concepts with sets of perceptual features. Based on this theory, an architecture for heterogeneous robots was developed [6]. Figure 1 presents a visualization of the architecture and how and what the robots communicate with each other.
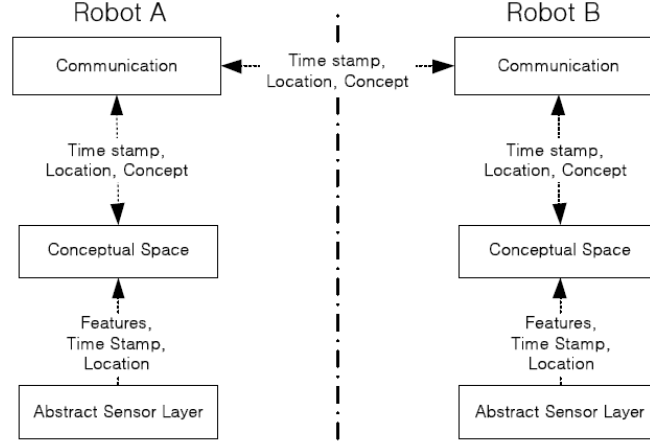

Figure 1. The architecture has three components: the communication module, conceptual space, and abstract sensor layer.

Each of the sensors provides raw sensor data relating to the intrinsic properties of the observed objects. This sensory data is processed within the Abstract Sensor Layer (ASL) to obtain relevant perceptual features, which are then mapped into the respective domains that define the Conceptual Space. As per Conceptual Spaces theory, each domain is composed of quality dimensions that represent various perceived qualities of situations or objects. Because these quality dimensions are metric, the similarity between the qualities of a detected object and of the concept under study can be easily calculated. Thus each domain verifies how similar the respective perceptual feature of the detected object is to the same feature of, in this case, the concept of a biohazard. The more similar the features are, the higher the probability that the detected object is indeed a biohazard.

2.1 Conceptual Space Definition

A conceptual space is made up of a symbol space and a concept space (Figure 2). In the symbol space, each symbol defines a different concept. Inside the concept space, a concept has several domains that distinguish it from other concepts. Thus, a specific concept is represented as a set of regions inside the domains. Each domain is composed of quality dimensions that represent the perceptual features obtained from the sensors. Their function is to represent various qualities of situations or objects. As stated earlier, the quality dimensions of the domains are metric, thus determining the similarity between a given instance of an object and a defined (or learned [7]) concept is straightforward.
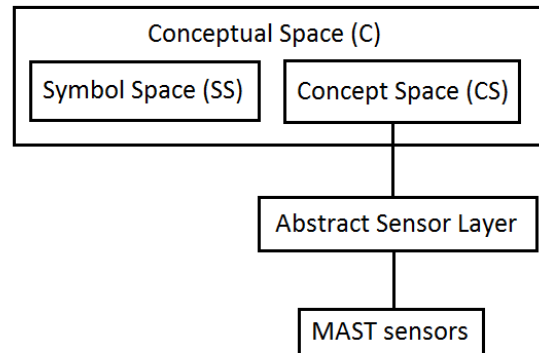

Figure 2. Schematic of a Conceptual Space and its components.

Different sensors feed raw sensor data into each individual robot's Abstract Sensor Layer (ASL). Remember that the robots do not share the same sensors and perceive the world in radically different ways. The ASL then processes the data and makes available perceptual features that are useful to identify/classify different objects. When an object property is detected, an instance of the relevant perceptual feature is compared to the already defined abstract concept prototype and associated probability distribution defining the concept. Depending on the probability of how similar that instance is to the concept, either an allocentric or egocentric location of the object in question (the candidate concept) is transmitted to the rest of the team for confirmation. In this initial research, without loss of generality, all experiments were made with the end goal of detecting a biohazard threat in a given environment. All robots, each mounted with widely heterogeneous sensors, must collectively achieve a consensus in determining if a detected object is considered as a biohazard threat or not. No individual robot has sufficient sensing capability to achieve the task by itself.

2.2 Use of the Conceptual Space

Consider how to represent an apple in a conceptual space. As humans, we can identify an apple by its intrinsic properties that, all together, specifically define an apple and nothing else (e.g. color, shape, texture, taste). As mentioned before, each property is represented by a region in a given domain. Thus, robots can use these regions (as we use the properties) to identify/classify a concept. The most representative member of a region is defined as its prototype. Thanks to the metric world of the domains, when a robot detects the color of an apple, sensor data from the camera is represented as a point in the quality dimensions, and the Euclidean distance between the instance and the prototype can be easily calculated. The closer the instance is to the prototype, the more likely it is to have the same color property as an apple. This analysis is done for all domains (shape domain, taste domain, etc.). It will be shown in Section 4 that, given a likelihood estimation, a likelihood value for an instance can be obtained based on the Euclidean distance between the instance and the center of the different regions that defines the properties of a given concept. The higher this likelihood value is, the more likely the entity in question is to be classified as an instance of the underlying concept.

3. SURROGATE MAST SENSORS

Before mapping sensor data into the conceptual space [4], features of interest are extracted from the sensors first into the Abstract Sensor Layer (see [6] for architectural details). Most of the sensors to be in used in MAST robots are still in the process of being developed. For this reason, surrogate sensors with similar or analogous functionalities are used to supply the robots with real-world data to verify our work (Figure 3). Table 1 compares the capabilities of the envisioned sensors and the surrogate sensors currently used.

Table 1: MAST Sensors and their Surrogates

MAST sensor	Measurements		Surrogate Sensor	Measurements
Hot-wire Air Flow	• Air flow velocity • Air flow direction		Wind sensor	• Air flow velocity
Micro Gas Chromatograph	• Identification of Chemical Species • Concentration of Chemical Species		CO_2 sensor	• CO_2 concentration
Scanning laser range finder	• Distance • Feature point for shape identification		Hokuyo laser range finder	• Distance (0– 4m)
IR Thermal Camera	• Temperature		RGB camera	• Temperature
Vision Sensor	• Color • Symbol detection		RGB camera	• Color (HSV) • Size

When biohazard materials are stored, one wants to be certain to store it safely; hence, it is logical to believe that there will be a negative airflow towards a biohazard container to keep it well ventilated. The surrogate airflow sensor from Modern Devices is capable of detecting wind and producing logarithmically corresponding voltage, but unlike the target HAIR sensor, this surrogate can only detect the wind flow

velocity in one direction. The surrogate sensor also responds to sideways wind flow, although more weakly. As a result, weak frontal wind and strong sideways wind cannot be distinguished from one another, which presents challenges in determining the airflow direction when using the surrogate sensor.
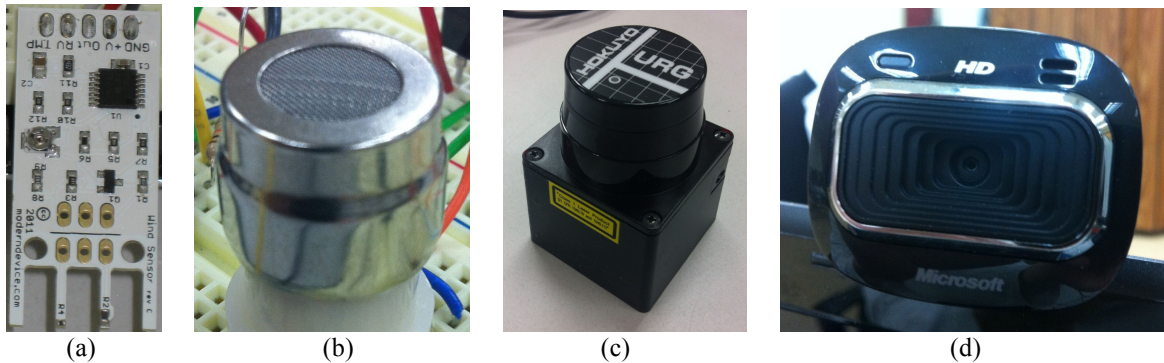

(a)   (b)   (c)   (d)

Figure 3: Surrogate Sensors. (a) Wind sensor (b) CO_2 sensor (c) Laser scanner (d) Web camera visual sensor

If it is possible to sense airborne biohazard materials at low concentrations, it will be strong evidence of a biohazard container kept in vicinity. Otherwise a swab sample analysis taken by a robot can serve as a means for positive identification. For our testing purposes, a carbon dioxide (CO_2) sensor acts as the surrogate Micro Gas Chromatograph, specifically the MG811 CO_2 sensor from Shitongda Electric Co. It is capable of detecting CO_2 concentration of 350 – 10000ppm, and outputs corresponding analog voltage between 30 – 50mV. It has good selectivity to CO_2 and is simple to set up and start sensing CO_2 concentrations through an analog-to-digital converter (ADC). However, due to its wide sensing range but small output range, it needs an appropriate voltage amplifier. A non-inverting voltage amplifier has been placed between the sensor output and ADC input to address this problem. The sensor has been tested by exposing it to fumes from dry ice. Currently only coarse measurements indicating degrees of CO_2 concentration can be taken with this sensor. There are other candidates for surrogate Micro Gas Chromatograph, but MG811 was chosen for its price and ease of use. We intend to replace the surrogate sensor with a more sophisticated gas sensor in the future, perhaps for several different gases.

Laser range finders supply autonomous robots data to do many things, including navigation, obstacle avoidance, and feature detection. The Hokuyo URG-04LX-UG01 scanning range finder serves as the surrogate sensor for both the scanning laser ranger finder and millimeter-wave radar. It has a scanning distance of up to 4 meters, 240° scanning range, lightweight, low power consumption, and angular resolution of 0.352°. It is powered and interfaced through USB. Also, a driver is available in ROS, making it easier to interface in Linux.

It is reasonable to believe that biohazard materials will be kept inside a container of certain specific shapes and sizes, as there is some tendency towards standardization. It might also be the case that those containers bear the standard markings of biohazard material. A vision sensor is required to look for these features. A normal USB webcam serves as the surrogate sensor for the micro-vision MAST sensor. The model chosen is a Microsoft Lifecam HD-5000. It was chosen for its color quality and ease of interface with Linux. OpenCV is used to extract color blobs from objects of interest, and analyze its color (HSV space), blob shape, and blob size [13].

Work is currently ongoing to simulate temperature data from RGB camera for the surrogate IR Thermal Camera. The same vision camera will be used for the surrogate IR Thermal Camera as for the surrogate Vision Sensor, but different processing algorithm will be implemented to mimic IR Thermal Camera to extract object temperature data. Real IR thermal imaging cameras have prohibitively high costs, even those with very low resolution, so data from IR Thermal Camera are being emulated with a normal camera for the time being.

3.1. Implementation of Abstract Sensor Layers for Surrogate Sensors

In the search and identification scenario, concepts are sought that indicate the existence of a biohazard, which is characterized by its associated container, temperature and airflow storage criteria, and chemical signature. To achieve this end, before mapping sensor data into the conceptual space, features of interest are extracted

from the sensors and deposited within the Abstract Sensor Layer. Table 2 lists the MAST sensors, their corresponding surrogate sensors, and the features extracted by the Abstract Sensor Layer. In our current implementation, sensor-specific data structures are populated with this extracted feature data. Sensor data structures contain the features shown in Table 2.

Table 2: Perceptual Features produced by sensors for storage in ASL

Sensor	Surrogate Sensor	Features
Hot-wire Air Flow	Wind sensor	Air flow velocity (m/s)
Micro Gas Chromatograph	CO_2 sensor	CO_2 concentration (digital voltage)
Scanning laser range finder	Hokuyo laser range finder	Data about circular or cornered objects in sight (number, coordinates to the center, and geometrical properties)
IR Thermal Camera	RGB camera	Average temperature of the object of interest
Vision Sensor	RGB camera	Data about 4-sided objects of certain color in sight (number, size of the blob, and HSV values)

Since a surrogate IR Thermal Camera has not been completed yet, the detection algorithm for surrogate IR Thermal Camera remains to be implemented at the time of publication. The Abstract Sensor Layer for surrogate wind sensor is a null function; the voltage level from the surrogate sensor is automatically converted to airflow velocity at hardware level with a conversion function that is specific to that sensor, before Abstract Sensor Layer operates on it. Thus, the Abstract Sensor Layer does not have to do other feature detection tasks other than simply filling in the data structure for the wind sensor with the actual sensor's output. The surrogate Micro Gas Chromatograph similarly has a null function for its Abstract Sensor Layer.

The scanning laser ranger finder has an abstract Sensor Layer algorithm that extracts various features from a single scan data, based on an algorithm introduced in [15]. Using the distance and angular displacement data of individual points from one set of scan data, it can be turned into an egocentric 2-D plane with individual points having the same distance from the origin and angular displacement from a certain reference angle, e.g. the x-axis. Adjacent points with a difference in distance above a certain threshold are considered different segments, and these segments are marked accordingly. Then inscribed angles for each scan points are calculated. By processing these inscribed angles statistically, the algorithm offers an accurate feature analysis of what it sees.

In accordance with the scenario of looking for possible containers of biohazard materials, qualities that biohazard containers are likely to have are sought after. For a scanning laser range finder, the concept of the shape of a container is of value. In our implementation, the algorithm only looks for circular objects, or objects with corners, which could possibly be the size and shape of a container. The Abstract Sensor Layer for searches for all circular/cornered objects in its laser scanning range. Then different types of features are calculated for different shapes of container candidates. For example, a scan data set is calculated that contains circular object, i.e., the number of those circles, the egocentric coordinates to their centers, distance to their centers, their radius and curvature. Curvature here is defined with respect to the second derivative calculated using discrete points. It is defined for circular and squared readings alike, and expresses how round a given segment of a sensor reading is, but it is not the inverse of radius.

The Abstract Sensor Layer for the surrogate Vision Sensor consists of algorithms to process the visual data to extract data about objects. Color blob detection algorithm is used to segment blobs of certain colors of interest from an incoming image. Shape detection algorithm is then used to look for blobs of certain shape, such as rectangular blobs. Once color blobs that match these criteria are found, the Abstract Sensor Layer populates the data structure for Vision Sensor with a number of such objects, and their HSV values are calculated from the cameras RGB values. Currently, OpenCV is used to implement these algorithms. It will be a significant addition to incorporate biohazard symbol (Fig. 5 left) detection to the Abstract Sensor Layer for the Vision Sensor, but has not been incorporated in this research yet.

4. IMPLEMENTATION

All experiments were made using the *MissionLab*[1] mission specification system [3,5,11]. This software was used to code algorithms that are capable of implementing the described architecture and determining if it is useful for knowledge sharing in this context. The open source command-line program *gnuplot* was used to plot an object's features into the respective domains. These plots serve as a visual representation of the respective domains in a given Conceptual Space.

As mentioned in Section 3, the following sensors are used: a wind sensor, a webcam for color detection, a carbon dioxide (CO_2) sensor, and the Hokuyo laser range finder. These sensors serve as surrogates for the MAST-specific sensors under development by the MAST Microsystems group at the University of Michigan. It is intended that in the future these sensors will be replaced by the MAST-specific ones and others may be added as well.

Each sensor provides raw sensor data relating to the intrinsic properties of the observed objects. This data is then processed in the ASL to obtain relevant perceptual features, which are then mapped into the respective domains.

4.1 Conceptual Space Designs

As mentioned previously, each conceptual space is composed of several domains that contain a set of regions that define a specific concept. The designed domains depend on the sensors mounted on each robot. For each domain, the quality dimensions (axes) are the perceptual features obtained from the ASL which are then stored in a database. For example, after processing the webcam's raw data, the ASL generates HSV values for a detected object's color and plots them in the respective domain. Similarly, for the Hokuyo scanner, curvature and radius values of a detected object are generated and plotted into the respective domain. For the wind sensor and the CO_2 sensor: airflow velocity and CO2 readings are generated respectively. Figure 4 provides a visual representation of these designed domains with their respective quality dimensions.
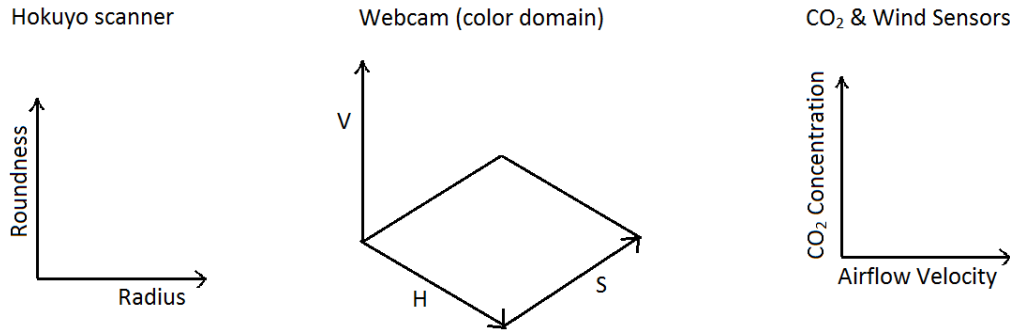

Figure 4. Implemented domains for four MAST sensors.

Both the Hokuyo scanner and the webcam have their own domain with their respective quality dimensions. It is important to mention that the CO_2 and wind sensors are independent of each other. They are shown in the same domain for simplicity at the time of classifying an instance. For both the CO_2 reading and the airflow velocity, arbitrary thresholds are selected. For example, an instance with CO_2 intensity below the selected threshold is disregarded and considered to have zero probability of matching the property. Above the threshold, the higher the CO_2 concentration is, the more likely it is to be a biohazard. For this project, dry ice is used as a source of CO_2 to represent a chemical signature of a potential biohazard. In addition, it is assumed that a biohazard will have a negative airflow associated to it (meaning that there is air flowing away from the object), which is usually a safety requirement for storage. This information is used to identify the presence of a potential biohazard.

4.2 Defining Properties as Gaussian Mixture Models

In a given conceptual space, each domain contains different regions that represent the concept's intrinsic properties. Each concept can be defined/identified by these properties. For example, an apple can be defined by its color (red or green), its texture (hard of soft for rotten apples), its shape, and its taste. Sometimes, a

---

[1] *MissionLab* is freely available for research and educational purposes at: http://www.cc.gatech.edu/ai/robot-lab/research/*MissionLab/*.

given property cannot be defined by a single region (an apple's color property can't be defined just as red). Therefore, the respective property region cannot be defined with a single Gaussian. This is why a Gaussian Mixture Model (GMM) is used to represent several regions for a given property.

Previous work [7,10] has shown that the mixture regions can be obtained by training the GMMs using different data sets. For this project, we obtain the model parameters by experimentally sensing sets of positive and negative instances. Figure 5 presents the objects used that are considered as positive instances of biohazard containers. Tables 3 and 4 summarize the positive and some negative instances used in the experiments.

Figure 5. Objects used as positive instances that represent a biohazard threat. From left to right: a) biohazard bucket, b) gray rectangular biohazard container, and c) red rectangular biohazard container.

Table 3. Positive instances used to represent a potential biohazard threat.

Positive Instances	Microsoft Life Webcam	Hokuyo Laser Range Finder	CO_2 Detector	Wind Sensor
1	Red	Cylindrical	Present	Present
2	Red	Rectangular	Present	Present
3	Gray	Rectangular	Present	Present

Table 4. Some negative instances used to verify that the algorithm can classify objects correctly.

Negative Instances	Microsoft Life Webcam	Hokuyo Laser Range Finder	CO_2 Detector	Wind Sensor
1	Green	Cylindrical	Absent	Absent
2	Green	Cylindrical	Present	Absent
3	Red	Rectangular	Absent	Absent
4	Blue	Cylindrical	Present	Present

Table 5. Prototypes for each region that defines the biohazard bucket.

Domains	Quality Dimensions	Prototypes of each region	Covariance Matrices
Wind sensor and CO_2 detector	Airflow velocity (m/s) and CO_2 concentration (k ppm)	(0.4, 2.5)	$\begin{bmatrix} 0.95 & 0 \\ 0 & 90 \end{bmatrix}$
Hokuyo Laser Range Finder	Radius(m) and Curvature (1/m)	(0.15, 0.3)	$\begin{bmatrix} 50 & 1 \\ 1 & 40 \end{bmatrix}$
Microsoft Life Webcam	HSV values	(177, 192, 255)	$\begin{bmatrix} 0.001 & 0 & 0 \\ 0 & 0.0005 & 0 \\ 0 & 0 & 0.002 \end{bmatrix}$

In a given domain, each region/property has a prototype. A prototype is the most representative value of each region. For each domain, Table 5 presents the prototypes of the regions that define the biohazard bucket (Figure 5).

A Gaussian Mixture Model is a parametric probability density function represented as a weighted sum of Gaussian component densities:

$$p(x|\theta) = \sum_{i=1}^{M} w_i * p(x|u_i, \Sigma_i) \qquad (1)$$

where x is a feature vector for a property, M is the number of Gaussian Models, and w_i is known as the mixing proportions. θ is a set containing all of the mixing proportions and model parameters:

$$\theta = \{w_i, u_i, \Sigma_i\}_{i=1}^{M} \qquad (2)$$

where u_i is the mean of the model, and Σ_i is a covariance matrix.

The model parameters needed to define a GMM can be obtained after running the Expectation Maximization (EM) Algorithm [2]. Given a set of data points, the algorithm groups different points into clusters and assigns each cluster the model parameters that separate it from the others. It alternates between estimating the association of the points to the clusters and updating the parameters of the clusters given the association.

For this project, each region is defined directly with the model parameters. The mean and the covariance matrix are defined by experimentally sensing the positive instances in Table 3 and mapping the features into their respective domains. The mean is equal to the prototype of the region – the most representative values of a cluster, and the covariance matrix determines how much the cluster stretches in the axes of the domain. In other words, it defines how far a detection can stray away from the center of a region and still remain a concept property. In a 2D domain, the covariance matrix is a symmetric 2x2 matrix and defines the convex regions as ellipses. Similarly, the covariance matrix is a symmetric 3x3 matrix and defines the convex regions as an ellipsoid for a 3D domain.

4.3 Classification of an Instance (Maximum Likelihood Estimation)

When a robot senses an object, it plots the instance into the respective sensory domain (which includes all mixture regions that define the positive detections). A Maximum Likelihood Estimation (MLE) [12] is obtained to determine the region to which each instance is more likely to be a member of. For a given domain, the likelihood of an instance relative to all the regions is based on the Euclidean distance between said instance and the mean (prototype) of each region. In addition to the MLE, we also use the following equation to determine how likely it is for the instance to be a part of the selected region:

$$c(k) = \sum_{i=1}^{n} a(k, i) \cdot s[p(k, i), f(k, i)] \qquad (3)$$

where s(p(k,i),f(k,i)) is the similarity between the ith property p of the kth concept and the ith feature f of the detected object. The similarity between two points is defined as the Euclidean distance between them:

$$s(a, b) = [1 + d(a, b)]^{-1} \qquad (4)$$

where d(a,b) is the Euclidean distance between a and b.

For this research, using the MLE together with the similarity value provides a better estimation for the detection of a potential biohazard versus calculating only the similarity between an instance and the prototypes of each region. When calculating similarity values, the actual region around its prototype is not taken into consideration. When using MLE, the covariance matrices and mean values take into account the convex region that was chosen to define the properties of the biohazard concept. Moreover, using only the MLE determines how likely an instance is of being a member of one region versus another. It doesn't state how likely it is of being a member of the selected region. This is why the combination of the similarity value and the MLE proves to be useful. Finally, it's important to mention that the logarithm of the likelihood is used rather than the likelihood itself because likelihoods, being products of the probabilities of many data points, tend to be very small. In contrast, the logarithm of the likelihood, which sums instead of multiplying, tends to grow.

5. EXPERIMENTAL RESULTS

5.1 Experimental Procedure

Several experimental tests were performed both in simulation and with real sensor data in order to demonstrate the value of the conceptual spaces approach in MAST relevant scenarios, specifically in the case of identification of a biohazard threat. These preliminary experiments consist of a stationary robot directly viewing a given object possibly representing the concept in question. However, the end goal is to extend the conceptual spaces approach for knowledge sharing among a team of widely heterogeneous robots. Future experiments will extend to multiple robots searching a given environment for a potential biohazard threat.
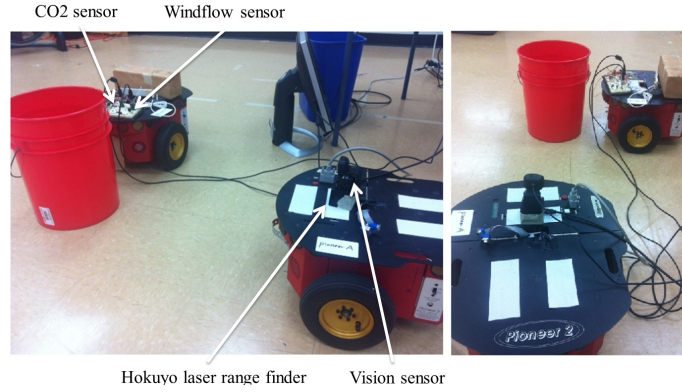

Figure 6. Basic experimental setup.

Figure 6 shows the basic configuration for all robotic experiments. The robot closest to the object (red biohazard bucket) is used for support of the CO_2 and wind sensors given that their range of measurement is limited. The goal is to have a consensus between all the domains and determine if the detected object fits the concept of a biohazard threat or not. All sensors/domains were controlled by a single centralized computer. In future experiments, the domains will be separated between two or more robots with each robot separately. One of the robots will then be assigned the Hokuyo scanner and webcam domains (a notional flyer), and the second robot will be assigned the CO_2 & Airflow Velocity domain (a notional crawler).

The main experiment is as follows: an object (positive or negative instance of a biohazard threat) is placed directly in front of the sensors. Relevant perceptual features are extracted from the ASL for the three biohazard concept domains shown in Figure 3. These features are then mapped into the respective domains. A MLE is calculated to determine the region to which an instance is more likely to belong to. If and only if the concept value (eq. 3) between the instance and the selected region is greater than the established threshold that defines a biohazard, then will all the domains come to a consensus and classify the detected object as a potential biohazard. If so, an alert message is sent to notify the user. This message contains a time stamp, the robot id, the distance between the robot and the detected object, and the robot heading with respect to the position of the object.

5.2 Simulation Testing

To test the system, two simulated runs were made using the implemented code in *MissionLab*. The runs were made based on the positive and negative instances presented in Tables 3 and 4. For the positive instance, random data was generated around the respective prototypes that define the selected object. For example, when simulating the biohazard bucket, random data is generated around the prototypes of each domain (Table 5) plus some added noise. When simulating a negative instance, random data is generated around the measured values for each domain (e.g., for the Hokuyo domain, the generated data involves the measured radius and curvature plus some added noise). Since the ASL data was generated near predefined points, these simulated runs are considered to be ideal and are used to test the functionality of the code prior to deployment on the robots.

Tables 6 and 7 show 5 data points generated from the ASL for the biohazard bucket (positive instance) and the blue cylindrical container (negative instance) respectively. The information shown in these tables are the perceptual features used to obtain the MLE values and analyze the detected object. Additional perceptual features can be extracted from the ASL. For example, the distance and the angle between the robot and the

target object can be extracted from the Hokuyo domain. Even so, this additional information isn't used for the identification, but for the localization of the detected object in the event that the robots classify it as a biohazard threat. Tables 8 and 9 show the resulting MLE values that correspond to the data points in Tables 6 and 7. Each data point generates a likelihood value for each region per domain. The likelihood values are used to determine to which region an instance is more likely to be a member of. Tables 8 and 9 also show the calculated similarity values obtained from equation (3) for each instance. These values are the ones used in the classification of the detected object. For these simulated experiments, a threshold equal to 35 was arbitrarily selected, indicating that all instances with a similarity value above 35 are considered a potential biohazard. Figures 6 and 7 show a given instance plotted into all domains at time t for the biohazard bucket and the blue container respectively. These figures illustrate how the data points extracted from the ASL are mapped into their respective plots.

Table 8 shows that the biohazard bucket is indeed classified as a potential biohazard threat given the following: 1) the likelihood values indicate that a selected measured instance will map into the property regions that define the concept of a biohazard, and 2) the calculated similarity values are above the selected threshold. Figure 6 supports the conclusion obtained from Table 8. It can be seen that the selected measured

Table 6. Five data points generated from the ASL for the biohazard bucket (positive instance) for all domains.

Hokuyo Scanner Domain		Vision Domain			CO$_2$ and Wind Sensors Domain	
Radius (m)	Curvature (1/m)	H	S	V	Windflow (m/s)	CO$_2$ Concentration (k ppm)
0.101	0.410	178	215	207	0.49	2.687
0.184	0.363	175	213	205	0.18	2.309
0.159	0.441	179	212	205	0.53	2.291
0.183	0.431	175	215	208	0.16	2.603
0.165	0.422	178	216	206	0.23	2.536

Table 7. Five data points generated from the ASL for the blue container (negative instance) for all domains.

Hokuyo Scanner Domain		Vision Domain			CO$_2$ and Wind Sensors Domain	
Radius (m)	Curvature (1/m)	H	S	V	Windflow (m/s)	CO$_2$ Concentration (k ppm)
0.162	0.365	114	212	87	-0.08	1.23
0.165	0.403	114	211	86	-0.18	1.04
0.192	0.373	114	209	86	0.35	0.83
0.177	0.427	117	211	86	-0.10	1.15
0.194	0.380	114	211	85	-0.06	1.07

Table 8. Likelihood values obtained from the MLE implemented algorithm for all domains for biohazard bucket.

Hokuyo Scanner Domain		Vision Domain (x10^{11})		CO$_2$ and Wind Sensors Domain	Final Similarity Value
Region1	Region2	Region1	Region2	Region1	
-8.112	-26.020	-6.923	-0.0002	-48.720	48.230
-6.932	-18.010	-6.729	-0.0003	-261.226	42.976
-8.819	-22.933	-6.726	-0.0006	-93.599	39.910
-8.565	-20.878	-6.901	-0.0004	-307.292	36.476
-8.206	-21.646	-6.963	-0.0004	-157.698	36.749

Table 9. Likelihood values obtained from the MLE implemented algorithm for all domains for blue cylindrical container.

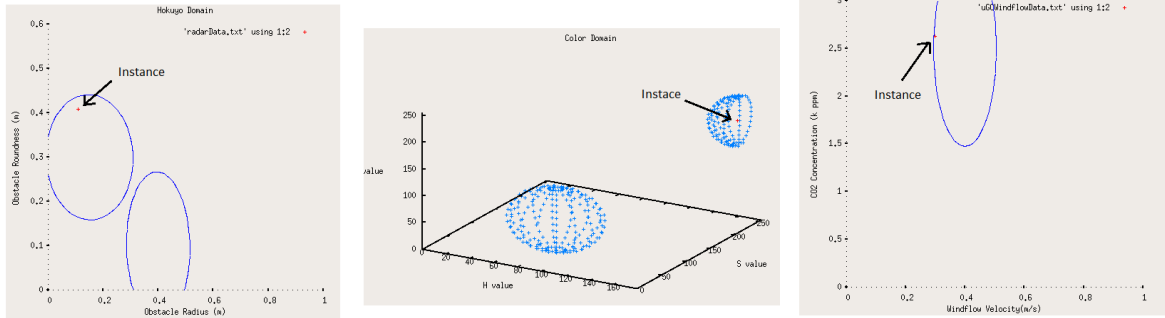| Hokuyo Scanner Domain		Vision Domain (x10^{11})		CO$_2$ and Wind Sensors Domain	Final Similarity Value
Region1	Region2	Region1	Region2	Region1	
-6.870	-19.516	-4.971	-0.553	-1306.86	31.618
-7.673	-20.820	-4.912	-0.559	-1893.01	31.659
-7.159	-17.896	-4.799	-0.561	-173.09	32.341
-8.404	-21.078	-4.922	-0.541	-1420.95	33.762
-7.308	-18.046	-4.911	-0.565	-1231.67	31.349

Figure 6. An instance represented as a red dot is mapped into all the domains for the simulated experiment while looking at the biohazard bucket (positive instance).
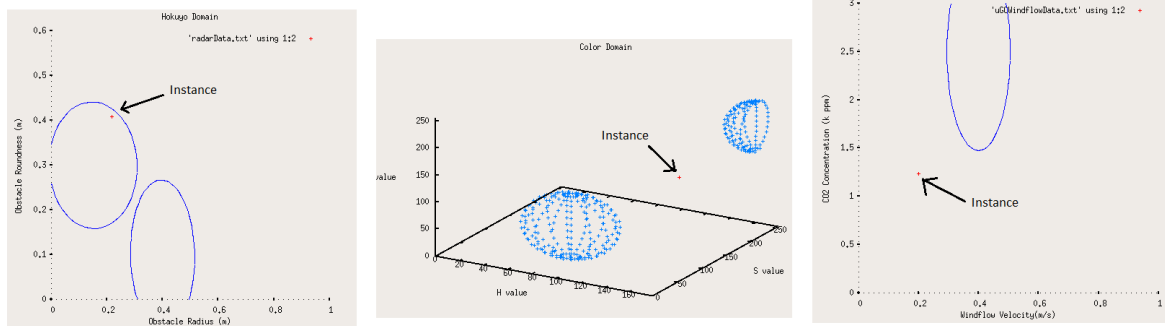

Figure 7. An instance represented as a red dot is mapped into all the domains for the simulated experiment while looking at the blue cylindrical container (negative instance).

instance is mapped directly into the constructed regions. For example, for the Color domain, Table 8 shows that the instance will be more likely a member of region 2 (defines the color red), than a member of region 1 (defines the color gray). This is illustrated in Figure 6 (Center).

Similarly, Table 9 shows that the blue cylindrical container is not classified as a biohazard threat. All the calculated similarity values are below the selected threshold. In addition, both the MLE values and Figure 7 show that the measured instance is not mapped into the regions that define a biohazard. For example, for the Color domain in Figure 7 (Center), the instance is seen between regions. Although the MLE analysis shows that it is more likely for the instance to be a member of region 2 than a member of region 1, it is not close enough to either one to be considered as a biohazard.

Note that for the Hokuyo domain, the measured instance for the blue container is inside region 1 (defines cylindrical objects). Although this domain suggests that the detected object is a potential biohazard, the other two domains deny it. This is a basis of conceptual space theory: making decisions based on the consensus from all available domains. We expand these concepts to using real surrogate sensors below.

5.3 Robot Experimental Testing

For the preliminary robot experimental testing, the ASL values are obtained from raw sensory data. When using actual sensors, there is much more to take into consideration. For example: contrary to the simulated experiments, at any given point in time the sensors may detect more than one object. In addition, not all sensors will detect all of the same objects. It may be that, in addition to the object placed in front of the robots, the Hokuyo scanner detects three more objects in the background while the webcam detects only one more object due to the established color thresholds. Moreover, it will be shown that, even though these objects were previously classified as positive or negative instances, the results of each run may present false positives. This is due to different ambient factors such as room lighting, sensory noise, and room temperature.

Figure 6 shows the experimental setup of the robots and the objects for each run. One of the robots is placed very close to the object given that the range of detection of the CO_2 is very limited. Note that, due to the difficulties of calibrating the sensor, readings for CO_2 concentrations are only meant to provide relative concentrations. Actual sensor output and interpreted sensor values are correlated, but the interpreted sensor values do not correctly represent the actual physical gas concentration. They are only given scale for the ease of interpretation. The case for the wind sensor is also similar.

Using the experimental configuration, three tests were conducted using real sensor data: 1) the biohazard bucket (positive instance), 2) the blue cylindrical container (negative instance), and 3) the gray squared container (positive instance) (See Tables 3 and 4). Tables 10-12 show the generated ASL values obtained from raw sensory data for the experiment runs made with the biohazard bucket, blue cylindrical container, and gray squared container respectively. Tables 13-15 show the resulting Likelihood values from the MLE, and calculated similarity values. Figures 8-10 show how a selected instance in time t is mapped into the respective domains for each experiment run. For these experimental runs using real surrogate sensors, the selected threshold for the similarity values was empirically set to 30 (the threshold was set lower than the simulation value of 35 due to consistently lower similarity values returned in the robot experiments. Learning techniques developed earlier in our laboratory could assist in threshold determination for concept recognition [7]). Any instance with a similarity value above 30 is classified as a potential biohazard.

Table 10. Five data points generated from the ASL for the biohazard bucket (positive instance) for all domains using real surrogate sensors.

Hokuyo Scanner Domain		Vision Domain			CO_2 and Wind Sensors Domain	
Radius (m)	Curvature (1/m)	H	S	V	Windflow (m/s)	CO_2 Concentration (k ppm)
0.126	0.356	178	233	223	0.378	1.500
0.126	0.250	179	235	224	0.394	1.600
0.125	0.241	177	241	219	0.349	2.100
0.127	0.382	0	255	137	0.439	1.900
0.126	0.250	179	235	224	0.394	1.600

Table 11. Five data points generated from the ASL for the blue cylindrical container (positive instance) for all domains using real surrogate sensors.

Hokuyo Scanner Domain		Vision Domain			CO_2 and Wind Sensors Domain	
Radius (m)	Curvature (1/m)	H	S	V	Windflow (m/s)	CO_2 Concentration (k ppm)
0.228	0.389420	113	206	204	0.368	2.400
0.227	0.397430	120	255	144	0.462	2.500
0.227	0.393	119	255	101	0.446	2.500
0.224	0.338	113	206	204	0.367	2.500
0.227	0.304	113	206	204	0.360	2.200

Table 12. Five data points generated from the ASL for the gray squared container (positive instance) for all domains using real surrogate sensors.

Hokuyo Scanner Domain		Vision Domain			CO_2 and Wind Sensors Domain	
Radius (m)	Curvature (1/m)	H	S	V	Windflow (m/s)	CO_2 Concentration (k ppm)
0.425	0	103	45	90	0.252	2.500
0.421	0	101	36	98	0.297	2.200
0.426	0	87	31	81	0.380	2.500
0.432	0	87	31	83	0.332	2.200
0.426	0	87	31	83	0.312	1.700

Table 13. Likelihood values obtained from the MLE implemented algorithm for all domains for biohazard container using real surrogate sensors.

Hokuyo Scanner Domain		Vision Domain ($x10^{11}$)		CO_2 and Wind Sensors Domain	Final Similarity Value
Region1	Region2	Region1	Region2	Region1	
-6.785	-21.792	-8.347	-4.337	-62.171	32.528
-6.690	-18.705	-8.511	-5.240	-49.238	31.810
-6.826	-18.598	-8.775	-7.712	-26.831	31.030
-7.237	-22.725	-8.447	-0.290	-32.093	30.732
-6.690	-18.705	-8.511	-0.0524	-49.238	31.810

Table 14. Likelihood values obtained from the MLE implemented algorithm for all domains for the blue cylindrical container using real surrogate sensors.

Hokuyo Scanner Domain		Vision Domain ($x10^{11}$)		CO_2 and Wind Sensors Domain	Final Similarity Value
Region1	Region2	Region1	Region2	Region1	
-7.900	-16.575	-5.808	-2.113	-9.94	27.042
-8.069	-16.948	-8.096	-4.266	-24.213	33.617
-7.985	-16.751	-7.800	-6.119	-14.999	19.885
-7.052	-14.855	-5.808	-2.113	-9.661	17.152
-6.926	-13.688	-5.808	-2.113	-17.461	27.170

Similar to the simulated experiments, the MLE likelihood values and the calculated similarity values (Tables 13, 14, and 15) are both used, and the plotted domains (Figures 8, 9, 10) to classify the detected object as a biohazard or not. For example, for the run made with the gray squared container, it can be observed in Figure 10 that the measured instance belongs to all the property regions that define a biohazard. For the CO_2 and wind flow domain, the measured instance is plotted directly into the region that defines the correct wind flow velocity and a significant amount of CO_2 is present.

Table 15. Likelihood values obtained from the MLE implemented algorithm for all domains for the gray rectangular container using real surrogate sensors.

Hokuyo Scanner Domain		Vision Domain (x10^{11})		CO$_2$ and Wind Sensors Domain	Final Similarity Value
Region1	Region2	Region1	Region2	Region1	
-25.590	-7.257	-0.026	-3.466	-119.798	30.773
-25.350	-7.226	-0.0435	-3.749	-64.543	31.449
-25.608	-7.260	-0.021	-4.145	-6.081	29.942
-25.938	-7.310	-0.023	-4.132	-33.728	31.864
-25.626	-7.262	-0.023	-4.132	-80.383	31.864

Figure 8. An instance represented as a red dot is mapped into all the domains for the simulated experiment while looking at the biohazard bucket (negative instance) using real surrogate sensors.
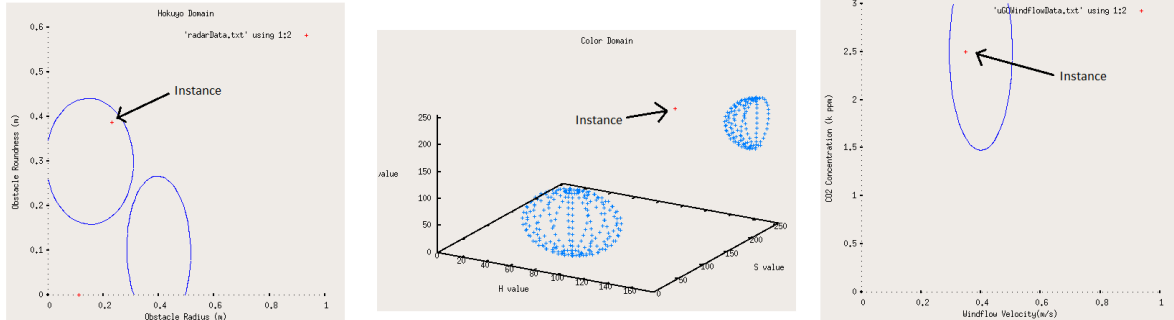

Figure 9. An instance represented as a red dot is mapped into all the domains for the simulated experiment while looking at the blue cylindrical container (negative instance) using real surrogate sensors.
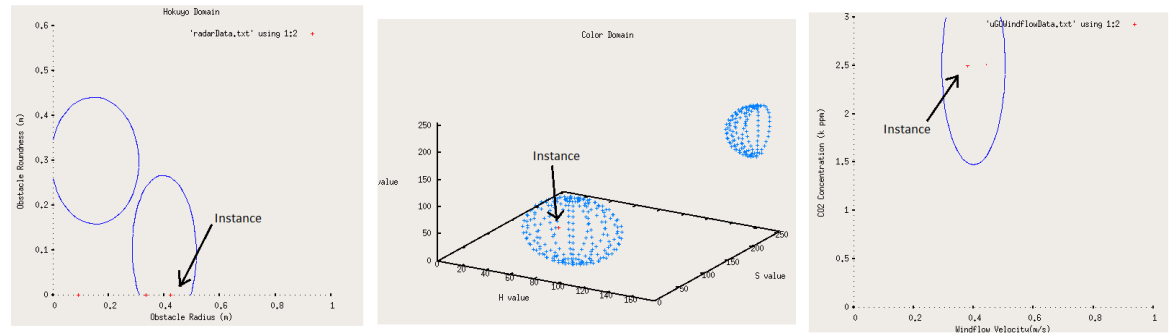

Figure 10. An instance represented as a red dot is mapped into all the domains for the simulated experiment while looking at the gray squared container (positive instance) using real surrogate sensors.

Figure 9 shows an example of how the blue cylindrical container may result in a false positive. Even though, for the Color domain, the measured instance is far away from both property regions, for the Hokuyo, and CO_2 and Wind domains, the measured instance is mapped directly into the regions that define a potential biohazard. In terms of the algorithm, the detected object has similar radius and curvature values as the defined biohazard bucket (Figure 9(Left)). It also has a considerable high concentration of CO_2 present and an associated wind velocity similar to the established prototype of the respective region. Equation (3) introduces a weighting value for each available domain. Given that having a high concentration of CO_2 is more significant the correct container color in terms of defining a biohazard concept, a higher weight value is assigned to the CO_2 and Wind domain. Thus, the presented measured instance is classified as a biohazard and, in this case, identified as a false positive (e.g. Table 14 Row #2).

As mentioned earlier, some domains may sense multiple objects as candidate concepts. For these preliminary experiments, given that we are trying to analyze only one object at a time, we assume that the relevant point is the one closest to the concept region. For example, in Figure 10 (Left), the Hokuyo scanner sensed three different objects. Given that the squared container is being observed, for which its width was previously measured, it is safe to assume that the relevant point is the one at radius approximately equal to 0.4m (the same as the measured value for width).

6. CONCLUSIONS

This paper presents the transition from the theoretical research developed earlier (e.g., [6-10]) to a practical working architectural implementation of Gardenfors conceptual spaces to a team of completely perceptually heterogeneous robots. Using sensors being developed by the Army's Microautonomous System Technology program and their surrogates, the abstract sensor layer (ASL) and conceptual space component of the overall system architecture has been implemented and tested, demonstrating the viability of this concept in the context of a biohazard search and detection mission.

Future work involves continued development and integration of sensor, both surrogate and actual MAST sensors alike, and the generation of team behavior based on the coordination required for all robots to share this knowledge among themselves.

ACKNOWLEDGMENTS

REFERENCES

[1] Aisbett, J. and Gibbon, G., "A general formulation of conceptual spaces as a meso level representation," Artificial Intelligence, pp. 189-232, (2001).

[2] Bilmes, J. A., "A Gentle Tutorial of the EM Algorithm and its Application to Parameter Estimation for Gaussian Mixture and Hidden Markov Models," International Computer Science Institute Berkeley CA, and Computer Science Division at U.C. Berkeley, (1998).

[3] Endo, Y., MacKenzie, D., and Arkin, R.C.,"Usability Evaluation of High-level User Assistance for Robot Mission Specification", IEEE Transactions on Systems, Man, and Cybernetics, 34(2), 168-180 (2004).

[4] Gardenfors, P., Conceptual Spaces: The Geometry of Thought, MIT Press, (2000).

[5] Georgia Tech Mobile Robotics Laboratory, MissionLab User Manual, Version 7.0, http://www.cc.gatech.edu/aimosaic/robot-lab/research/MissionLab/mlab_manual-7.0.pdf, (2007).

[6] Jung, H., Menon, A., and Arkin, R.C., "A Conceptual Space Architecture for Widely Heterogeneous Robotic Systems", Proc. 2nd International Conference on Biologically Inspired Cognitive Architectures (BICA 2011), Arlington, VA, November (2011).

[7] Kira, Z., "Inter-Robot Transfer Learning for Perceptual Classification", Proc. 9th International Conf. on Autonomous Agents and Multiagent Systems (AAMAS), *(*2010).

[8] Kira, Z., "Transferring Embodied Concepts between Perceptually Heterogeneous Robots", Proceedings IEEE/RSJ International Conference on Intelligent Robots and Systems (IROS), pp. 4650-4656, (2009).

[9] Kira, Z., "Mapping Grounded Object Properties across Perceptually Heterogeneous Embodiments", Proceedings of the 22nd International FLAIRS Conference, pp. 57-62, (2009).

[10] Kira, Z. Communication and Alignment of Grounded Symbolic Knowledge among Heterogeneous Robots, Ph.D. Dissertation, School of Interactive Computing, Georgia Institute of Technology, (2010).

[11] MacKenzie, D., Arkin, R.C., and Cameron, R., "Multiagent Mission Specification and Execution", Autonomous Robots, 4(1) 29-52, (1997).

[12] Myung, I. J., "Tutorial on maximum likelihood estimation," Journal of Mathematical Psychology 47, 90-100 (2003).

[13] OpenCV v2.3 documentation, http://opencv.itseez.com/ (Last day visited: March 7, 2012)

[14] Ulam, P., Kira, Z., Arkin, R., and Collins, T., "Mission Specification and Control for Unmanned Aerial and Ground Vehicles for Indoor Target Discovery and Tracking", SPIE Defense, Security, and Sensing, (2010).

[15] Xavier J., Pacheco M., Castro D., Ruano A., Nunes U., "Fast Line, Arc/Circle and Leg Detection from Laser Scan Data in a Player Driver" Proceedings of the 2005 IEEE International Conference on Robotics and Automation pp. 3930-3935, (2005).